

EXTREMES OF WAVE FORCES

By Mircea Grigoriu,¹ M. ASCE

ABSTRACT: Probabilistic descriptors are developed for Morison-type wave forces. They are based on the actual distribution of these forces and on the hypothesis that wave forces follow Gaussian distributions. The Gaussian hypothesis is characteristic of analyses based on statistical linearization. Results show that this hypothesis provides unsatisfactory estimates for the peak of wave forces during design storms. Both the mean and the variance of the peak wave force can be underestimated significantly when the Gaussian hypothesis is applied. It is assumed in the analysis that the wave particle velocity process follows a Gaussian distribution.

INTRODUCTION

According to Morison's equation, wave forces acting on cylindrical members have two components: drag forces, which depend nonlinearly on wave particle velocity, and inertia forces, which are proportional to wave particle acceleration (1,7,8,9,11,12). Wave forces are then non-Gaussian processes, although fluid velocities are assumed to follow Gaussian distributions. Yet, they are modeled by Gaussian processes when the analysis is based on statistical linearization because, in this approach, drag forces are approximated by linear functions of wave particle velocities (1,7,8,9,11).

The Gaussian hypothesis was examined extensively in the past, and probabilistic characteristics were developed for individual peaks of wave forces and the largest value of these forces during storms (1,7,9,10,12,13,14). The analysis of extreme wave forces was often based on the assumption that individual peaks are independent (1,12,13,14). Mean crossing rates of the wave force process (9,10) and simulation (7) were also applied to determine maxima of wave forces. Developments generally consider the case of small or nonexistent currents and assume that Morison's equation is valid.

This paper develops probabilistic descriptors for wave force processes characterized by Morison's equation, e.g., marginal distributions, mean crossing rates, and extreme value distributions, and further evaluates the Gaussian hypothesis. The descriptors are general and simple. They have closed forms for drag forces with or without current and involve a single numerical integration when drag and inertia forces are considered simultaneously. Results can be applied directly to the analysis of quasi-static response of offshore platforms when Morison's equation is valid.

WAVE FORCES

Let $Y^*(t)$ be the wave particle velocity at any time, t . It is assumed that $Y^*(t)$ is a twice-differentiable, stationary Gaussian process with pos-

¹Assoc. Prof. of Civ. Engrg., Cornell Univ., Ithaca, N.Y. 14853.

Note.—Discussion open until May 1, 1985. To extend the closing date one month, a written request must be filed with the ASCE Manager of Technical and Professional Publications. The manuscript for this paper was submitted for review and possible publication on April 27, 1984. This paper is part of the *Journal of Engineering Mechanics*, Vol. 110, No. 12, December, 1984. ©ASCE, ISSN 0733-9399/84/0012-1731/\$01.00. Paper No. 19330.

one such expression is $y_0^2 + 2y_0Y(t)$. It approximates the mean and the variance of the drag force by y_0^2 and $4\sigma_Y^2y_0 = 4\alpha^2y_0^2$. The corresponding dimensionless coefficients in Eq. 13 can then be approximated by $\xi \approx 1.0$ and $\zeta = 2\alpha$. From Table 1, the approach provides satisfactory second-moment descriptors for $X_1(t)$ when $\alpha \leq 0.5$.

Mean Crossing Rates.—The mean upcrossing rate of level x of $X_1(t)$, $v_1(x)$, can be obtained simply from developments in Appendix I related to nonlinear transformation of Gaussian processes. From Eq. 43 in this appendix and the observation that there is a one-to-one correspondence between drag forces and flow velocities, one finds

$$v_1(x) = \frac{1}{2\pi} \frac{\sigma_Y}{\sigma_Y} \exp \left\{ -\frac{1}{2} \left[\frac{\operatorname{sgn}(x) \sqrt{|x| - y_0}}{\sigma_Y} \right]^2 \right\} \quad (14)$$

$$\text{or } v_1(\bar{x}) = v_0 \exp \left\{ -\frac{1}{2} \left[\frac{\operatorname{sgn}(\xi + \zeta \bar{x}) \sqrt{|\xi + \zeta \bar{x}| - 1}}{\alpha} \right]^2 \right\} \quad (15)$$

$$\text{in which } v_0 = \frac{1}{2\pi} \frac{\sigma_Y}{\sigma_Y} = \frac{\sqrt{-\rho_Y''(0)}}{2\pi} \quad (16)$$

The standardized threshold, \bar{x} , gives the number of standard deviation, σ_1 , from m_1 to x and can be determined from

$$x = m_1 + \sigma_1 \bar{x} = y_0^2 (\xi + \zeta \bar{x}) \quad (17)$$

Let $v_1^G(x)$ be the mean upcrossing rate of level x of the drag force under the Gaussian hypothesis. According to this hypothesis, $X_1(t)$ is a Gaussian process. The corresponding mean upcrossing rate function has the expression (8,11)

$$v_1^G(\bar{x}) = \frac{1}{2\pi} \frac{\dot{\sigma}_1}{\sigma_1} \exp \left(-\frac{1}{2} \bar{x}^2 \right) \quad (18)$$

in which $\dot{\sigma}_1$ = the standard deviation of $\dot{X}_1(t) = dX_1(t)/dt$. From Eq. 4, the time-derivative of the drag force process is

$$\dot{X}_1(t) = 2[y_0 + Y(t)] \dot{Y}(t) \quad (19)$$

for all values of y_0 and $Y(t)$. Since $Y(t)$ and $\dot{Y}(t)$ are independent at any t , the process $\dot{X}_1(t)$ has the mean zero and variance

$$\dot{\sigma}_1^2 = 4\sigma_Y^2 y_0^2 (1 + \alpha^2) \quad (20)$$

The mean upcrossing rate in Eq. 18 can also be given in the form (Eqs. 13 and 20)

$$v_1^G(\bar{x}) = v_0 \frac{2\alpha \sqrt{1 + \alpha^2}}{\zeta} \exp \left(-\frac{1}{2} \bar{x}^2 \right) \quad (21)$$

The ratio between the exact and the approximate mean upcrossing rates, v_1 and v_1^G in Eqs. 15 and 21, has the expression

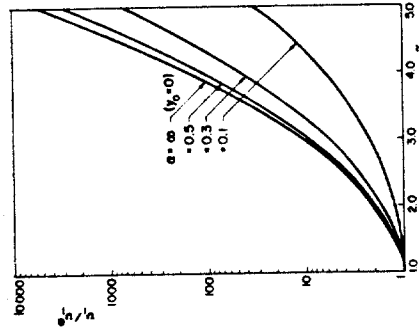


FIG. 1.—Ratio of Exact to Approximate Mean Upcrossing Rates of Drag Force

$$\frac{v_1(\bar{x})}{v_1^G(\bar{x})} = \frac{\zeta}{2\alpha \sqrt{1 + \alpha^2}} \exp \left\{ -\frac{1}{2} \left[\left(\frac{\sqrt{\xi + \zeta \bar{x}} - 1}{\alpha} \right)^2 + \bar{x}^2 \right] \right\} \quad (22)$$

for positive values of \bar{x} . Fig. 1 shows the variation of the ratio v_1/v_1^G in Eq. 22 with the standardized threshold, \bar{x} , for several values of α . Note that the Gaussian hypothesis results in unconservative approximations of the mean upcrossing rate. The degree of unconservatism increases with the threshold and the value of α (larger values of α correspond to smaller currents). For example, v_1/v_1^G is approximately 6.4 and 100 at $\bar{x} = 4.0$ when $\alpha = 0.1$ and 0.5, respectively. Note also that the ratio v_1/v_1^G is nearly independent of α and approximately equal to its value for $\alpha = \infty$ (zero current) when α exceeds 0.5. Values of α in excess of 0.5 are common in design.

Largest Value Distribution.—It is generally convenient to develop for design purposes other descriptors of the peak wave forces, in addition

to the mean upcrossing rate. Let $X_{1,r}$ be the maximum drag force during a storm of duration r and denote by

$$X_{1,r} = \frac{X_{1,r} - m_1}{\sigma_1} \quad (23)$$

The cumulative distribution function of $X_{1,r}$ at x can be determined from the probability that the drag force is smaller than x at $t = 0$, i.e., $X_1(0) \leq x$, and the number of upcrossings of threshold x of $X_1(t)$ during $[0, r]$, $N_r(x)$, is zero. This probability can be determined simply if it is assumed that the variables $X_1(0)$ and $N_r(x)$ are independent and the upcrossings of level x on $X_1(t)$ follow a Poisson process. The assumptions are satisfactory for relatively high thresholds (8,15) and provide the following expression for the distribution $F_{1,r}$ of $X_{1,r}$

$$F_{1,r}(\bar{x}) = F_1(\bar{x}) \exp [-(v_0 \sigma_1) \delta(\bar{x})] \quad (24)$$

This function depends on $\delta(\bar{x}) = v_1(\bar{x})/v_0$ with $v_1(\bar{x})$ in Eq. 15 and the

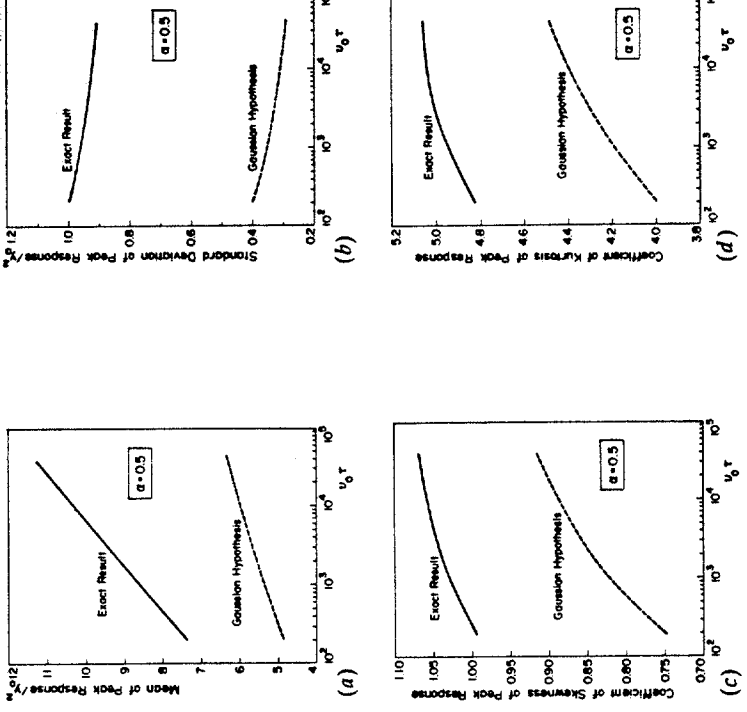


FIG. 2.—Exact and Approximate Probability Density Functions of Peak Drag Force

marginal distribution of $\hat{X}_1(t) = (X_1(t) - m_1)/\sigma_1$ which has the form

in which Φ = the cumulative distribution function of the standard Gaussian variable. The density of $\tilde{X}_{1,\tau}$, $f_{1,\tau}$, can be obtained by differentiating Eq. 24

$$f_{I,r}(x) = \delta(x) \exp [-(v_0 \tau) \delta(x)] \left\{ \frac{\zeta}{2\alpha \sqrt{2\pi |\xi + \zeta x|}} \right. \\ \left. + (v_0 \tau) \frac{\zeta \operatorname{sgn}(\xi + \zeta x) \sqrt{|\xi + \zeta x| - 1}}{2\alpha^2 \sqrt{|\xi + \zeta x|}} F_1(x) \right\} \dots \dots \dots \quad (26)$$

Similar considerations can be applied when Gaussian drag forces are postulated. In this case, the density $f_{1,r}^G$, of $\bar{X}_{1,r}$, has the expression

$$f_{f,r}^G(\tilde{x}) = \left[\frac{1}{\sqrt{2\pi}} + (v_0\sigma) \, \tilde{x} \Phi(\tilde{x}) \right] \exp \left\{ -\frac{\tilde{x}^2}{2} - (v_0\sigma) e^{-\tilde{x}^2/2} \right\} \dots \dots \dots \quad (27)$$

Fig. 2 shows the densities $f_{1,r}$ and $f_{1,r}^C$, with solid and dotted lines for $v_{\text{eff}} = 200$, 4,000, and 40,000. They are referred to as exact and Gaussian results. Note that the Gaussian hypothesis underestimates in the average the peak response

The densities in Eqs. 26–27 were used to determine by numerical integration the mean, the standard deviation, the coefficient of skewness, and the coefficient of kurtosis of the peak drag force. Fig. 3 shows the variation of these moments with v_{eff} for $\alpha = 0.5$. Similar results were found for other values of α . The means and the standard deviations plotted in this figure are divided y_0^2 . Note that the Gaussian hypothesis yields approximations which underestimate significantly the mean and the standard deviation of the peak wave force. For example, the exact values of the mean, the standard deviation, the coefficient of skewness, and the coefficient of kurtosis are $10.4 y_0^2$, $0.86 y_0^2$, 1.06 , and 5.05 for $\alpha = 0.5$ and $v_{\text{eff}} = 10,000$. These moments are approximated by $6.0 y_0^2$,

DRAG AND INERTIA FORCES

The general wave force in Eqs. 3-5 is examined in this section. Note that the drag and the inertia forces, $X_1(t)$ and $X_2(t)$, are independent at

any time t because $Y(t)$ and $\dot{Y}(t)$ are uncorrelated Gaussian processes. From Eqs. 3, 13, and 20, the mean and the variance of $R(t)$ are

$$m_r = \varepsilon'^2$$

(30)

$$\alpha_R^2 = (\zeta^2 + \beta^2) y_0^4$$

while the variance of the time-derivative of the wave force has the expression

These equations are valid when the current is not zero. When there is no current, $m_k = 0$, $\sigma_k^2 = 3\sigma_y^4 + \alpha_y^2$, and $\sigma_k^2 = 4\sigma_y^2\sigma_y^2 + \alpha^2\sigma_y^2$. The parameter β in Eq. 31 quantifies the importance of inertia force with respect to drag forces associated with the current and is equal to

is a derived parameter that has the following expression

$$= \frac{\sigma_Y'' a}{\sigma_Y' y_0} = \frac{\beta \sqrt{p_Y'''(0)}}{\alpha - p_Y''(0)} \dots \quad (34)$$

From Eqs. 33-34, β and δ depend on the correlation structure or, equivalently, the power spectral density of $Y(t)$. This dependence is examined in Table 2 for monochromatic, narrow-band, and wide-band wave particle velocities, $Y(t)$, for the case in which $\sigma_y^2 = 1.0$. Results show that at the ratio σ_y''/σ_y^2 depends weakly on the shape of the power spectral density of $Y(t)$. Thus, δ is primarily a function of the relative importance of inertia and drag forces, i.e., the ratio a/y_0 . The parameters, α , β , and γ can be determined simply from the ratio, a , between the inertia and drag coefficients, the current y_0 , and the spectral characteristics of flow velocity.

TABLE 2.—Spectral Characteristics of *W*.

One-sided spectral density of $Y(t)$				
$G_Y(\omega)$	σ_Y^2	σ_Y^2	σ_Y^2	σ_Y^2
(1)	(2)	(3)	(4)	(5)
$G_Y(\omega) = \begin{cases} 1.0, \omega = \omega_0 \\ 0.0, \text{otherwise} \end{cases}$	ω_0^2	ω_0^4	ω_0^4	1.0
$G_Y(\omega) = \begin{cases} 1, 0 \leq \omega \leq \omega_c \\ 0, \omega > \omega_c \end{cases}$	$\frac{\omega_c^2}{3}$	$\frac{\omega_c^4}{5}$	$\frac{3}{\sqrt{5}} = 1.3416$	
$G_Y(\omega) = \left\{ \begin{array}{l} \frac{1}{(\omega_b - \omega_c)}, \omega_c \leq \omega \leq \omega_b \\ \frac{\omega_b^2}{3}(p^2 + p + 1) \end{array} \right.$	$\frac{\omega_b^4}{5}(p^4 + p^3 + p^2 + p + 1)$	$\frac{3}{\sqrt{5}} \sqrt{p^4 + p^3 + p^2 + p + 1}$	$\frac{p^2 + p + 1}{\sqrt{5}}$	$1.0 \leq \sigma_Y^2 / \sigma_V^2 \leq 3/\sqrt{5}$
$= \begin{cases} 0.0, \text{otherwise } p = \frac{\omega_b}{\omega_0} \end{cases}$				$+ p + 1)$

Mean Crossing Rates.—The mean upcrossing rate of level r of $R(t)$, can be determined exactly from the mean rate at which the vector process $\{X_1(t), X_2(t)\}$ leaves the two-dimensional domain $\{(x_1, x_2) : x_1 + x_2 \leq r\}$ (3.16). For simplicity, v is approximated in this section from the point-crossing formula. According to this formula, v can be approximated by (6.17)

which f_i and ν_i denote the marginal density and the mean upcrossing rate functions of $X_i(t)$. The point-crossing formula has been applied successfully to the analysis of the combined effect of structural loads

The marginal density and the mean upcrossing rate functions of $X_1(t)$ in the drag force, are given in Eqs. 7 and 14. The corresponding functions of $X_2(t)$, the inertia force, can be determined simply because this process is Gaussian:

$$f_2^{**}(r) = \int_{-\infty}^{\infty} f_2(x_2) v_1(r - x_2) dx_2 + \int_{-\infty}^{\infty} f_1(x_1) v_2(r - x_1) dx_1, \dots \dots \dots \quad (35)$$

in which f_i and ν_i denote the marginal density and the mean upcrossing rate functions of $X(t)$. The point-crossing formula has been applied successfully to the analysis of the combined effect of structural loads.

The marginal density and the mean upcrossing rate functions of $X_1(t)$, the drag force, are given in Eqs. 7 and 14. The corresponding functions of $X_2(t)$, the inertia force, can be determined simply because this process Gaussian:

$$\langle \eta \rangle = \frac{1}{\sqrt{2\pi} a \sigma_\eta} \exp \left\{ -\frac{1}{2} \left[\frac{\eta}{a \sigma_\eta} \right]^2 \right\} \quad (36)$$

From Eq. 35, the mean upcrossing rate $v(r)$ can be approximated by

$$\text{which } \tilde{x} = (\omega - \omega_0)/\gamma \quad ; \quad \tau = \omega_0/\gamma \quad . \quad (38)$$

where $\tau = (\bar{v} - m_R)/\bar{u}_R$ with m_R and σ_R in Eqs. 30–31 and

$$\delta \exp \left\{ -\frac{1}{2} \left(\left(\frac{u-1}{u+1} \right)^2 + \left(\frac{\tilde{r} - \text{sgn}(u) u^2}{u+1} \right)^2 \right) \right\} d^u$$

$$d\tilde{r} = r/y_0^2 = \xi + \tilde{r}\sqrt{\xi^2 + \beta^2}. \quad (39)$$

The mean upcrossing rate of the wave force, when assumed to be a Gaussian process, can still be determined from Eq. 18, in which σ_R and σ_F are given by Eqs. 31 and 32. It has the expression

$$f) = v_0 \alpha \sqrt{\frac{4(1 + \alpha^2) + 8}{\alpha^2 - 1}} \exp\left(-\frac{1}{\alpha^2}\right) \dots \quad (40)$$

and involves only second-moment characteristics of the response and its second derivatives.

when inertia forces are dominant because, in this special case, the wave force is approximately a Gaussian process.

ACKNOWLEDGMENT

The writer wishes to thank R. Larrabee and E. Simiu for many enlightening conversations. This work was supported by the Minerals Management Service. The support is gratefully acknowledged.

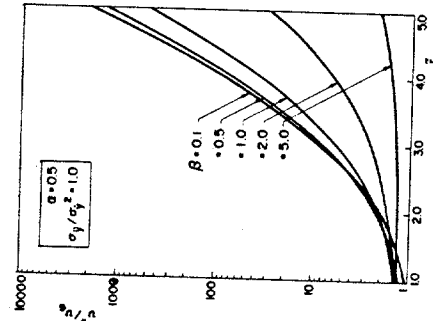


FIG. 4.—Ratio of Exact to Approximate Mean Upcrossing Rates of Drag and Inertia Forces

This result is applied to evaluate the Gaussian hypothesis although it involves approximations. However, the experience with the point-crossing formula (6.17) shows that errors associated with this formula are much smaller than those due to the Gaussian assumption (Fig. 1). Thus, it is considered that Eq. 41 provides a satisfactory base for the evaluation of the Gaussian hypothesis when both drag and inertia forces act simultaneously.

Fig. 4 shows the variation of v^*/v_G in Eq. 41 with \tilde{r} for $\sigma_Y^2/\sigma_{\dot{Y}}^2 = 1.0$ (i.e., monochromatic excitation), $\alpha = 0.5$ and selected values of β . The ratio v^*/v_G increases with the threshold but decreases with β . For small values of β drag forces are dominant and, as expected, v^*/v_G and ν_1/v_1^G in Fig. 1 are nearly equal. When inertia forces are significant β is large and the response follows approximately a Gaussian distribution. In this case, the Gaussian hypothesis is satisfactory ($v^*/v_G \approx 1.0$). Similar results have been found for other types of excitations, e.g., the narrow- and wide-band processes in Table 2.

The mean crossing rate functions developed in this section can be applied as in Eqs. 26–27 to determine probabilistic characteristics of the peak wave force during storms. However, such developments are not presented in this paper.

Journal

Exact and approximate descriptors were determined for the Morison-type wave forces and their peaks during design storms. The approximations were based on the hypothesis that wave forces follow Gaussian distributions. It was assumed that the wave particle velocity can be modelled by a Gaussian process.

Results show that the Gaussian hypothesis, which is characteristic to the statistical linearization method, yields unsatisfactory descriptors for the peak wave force. Both the mean and the variance of this variable are generally underestimated. The Gaussian hypothesis is acceptable only for a Gaussian process.

$$X(t) = g(Y^*(t)) \quad \dots \quad (43)$$

in which, g = a nonlinear transformation; and $Y^*(t)$ = a stationary Gaussian process with mean γ_0 and variance σ_y^2 . It is assumed that $Y^*(t)$ is differentiable and the variance of $dY^*(t)/dt$ is equal to σ_y^2 . The transformation g cannot generally be inverted over its entire domain of definition. However, it can be inverted over its intervals of monotony, D_i . In this intervals, $g = g_i$ is a monotonic function that takes on values in the range (a_i, b_i) . Fig. 5 shows this situation.

It can be shown (5) that the mean upcrossing rate of level x of $X(t)$, $v_X(x)$, can be obtained from the following equation:

卷之三

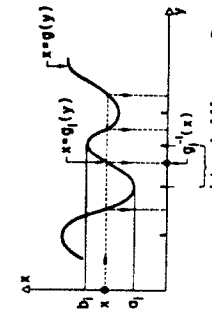
$$v_X(x) = \sum_i u_i(x) v_Y(g_i^{-1}(x)) \dots \quad (43)$$

in which, $u_i(x) = 1$ for x in (a_i, b_i) and is zero for arguments x outside this range. The function $v_Y(g_i^{-1}(x))$ denotes the mean upcrossing rate of level $g_i^{-1}(x)$ of $Y^*(t)$ and has the expression

卷之三

$$w_Y(g_i^{-1}(x)) = \frac{1}{2\pi} \frac{\sigma_Y}{\sigma_Y} \exp \left[-\frac{1}{2} \left(\frac{g_i^{-1}(x) - y_0}{\sigma_Y} \right)^2 \right] \dots \dots \dots \quad (44)$$

From Fig. 5, $X(t)$ upcrosses a threshold x when $Y^*(t)$ upcrosses any of the levels $g_i^{-1}(x)$. Thus, the number of upcrossings of level x of $X(t)$ during any period is equal to the total number of upcrossings of $Y^*(t)$ with respect to the levels $g_i^{-1}(x)$, for all values of i , over the same period. This observation can be used to write directly the results :- E-42



EIG E Nonlinear Transients 60

APPENDIX II.—REFERENCES

1. Borgman, L. E., "Statistical Models for Ocean Waves and Wave Forces," *Advances in Hydroscience*, Vol. 8, 1972, pp. 139-181.
2. Davenport, A. G., "Note on the Distribution of the Largest Value of a Random Function with Application to Just Loading," *Proceedings, Institution of Civil Engineers*, London, England, Vol. 28, 1964, pp. 187-196.
3. Grigoriu, M., "Mean Failure Rate for Structural Systems Subjected to Time-Dependent Loads," presented at the June 21-25, 1982, Ninth National Congress of Applied Mechanics, held at Ithaca, N.Y.
4. Grigoriu, M., "Dynamic Response of Offshore Platforms to Environmental Loads," *Proceedings of the 4th ASCE Specialty Conference on Probabilistic Mechanics and Structural Reliability*, American Society of Civil Engineers, Jan., 1984, pp. 115-118.
5. Grigoriu, M., "Crossings of Non-Gaussian Translation Processes," *Journal of Engineering Mechanics*, ASCE, approved for publication.
6. Larrabee, R. D., and Cornell, C. A., "Combination of Various Load Processes," *Journal of the Structural Division*, ASCE, Vol. 107, No. ST1, Paper 15999, Jan., 1981, pp. 223-239.
7. Larrabee, R. D., "Extreme Wave Dynamics of Deepwater Platforms," presented at the Aug., 1982, 3rd International Conference on Behavior of Offshore Structures, BOSS 82, held at Cambridge, Mass.
8. Lin, Y. K., *Probabilistic Theory of Structural Mechanics*, Robert E. Krieger Publishing Company, Huntington, N.Y., 1976.
9. Moe, G., and Crandall, S. H., "Extremes of Morison-Type Wave Loading on Simple Pile," *Transactions of the ASME*, Vol. 100, Jan., 1978, pp. 100-104.
10. Moe, G., "Long-Term Wave Force Statistics for a Vertical Pile," *Coastal Engineering*, Vol. 2, 1979, pp. 297-311.
11. Rice, S. O., "Mathematical Analysis of Random Noise," *Bell System Technical Journal*, Vol. 24, 1945, pp. 46-156.
12. Tickell, R. G., "Continuous Random Wave Loading on Structural Members," *The Structural Engineer*, Vol. 55, No. 5, May, 1977, pp. 209-222.
13. Tickell, R. G., "The Probabilistic Approach to Wave Loading on Marine Structures," *Mechanics of Wave-Induced Forces on Cylinders*, T. L. Shaw, ed., Pitman Advanced Publishing Program, San Francisco, Calif., 1979, pp. 152-178.
14. Tung, C. C., "Peak Distribution of Random Wave-Current Force," *Journal of the Engineering Mechanics Division*, ASCE, Vol. 100, No. EM5, Paper 10843, Oct., 1976, pp. 873-884.
15. Vanmarcke, E. H., "Structural Response to Earthquakes," *Seismic Risk and Engineering Decisions*, C. Lmitz and E. Rosenblueth, eds., Elsevier Publishing Co., Amsterdam, The Netherlands, 1976, pp. 287-337.
16. Veneziano, D., Grigoriu, M., and Cornell, C. A., "Vector-Process Models for System Reliability," *Journal of the Engineering Mechanics Division*, ASCE, Vol. 103, No. EM3, Paper 12981, June, 1977, pp. 441-460.
17. Winterstein, S. R., "Combined Dynamic Responses: Extremes and Fatigue Damage," *Research Report R80-46*, Department of Civil Engineering, Massachusetts Institute of Technology, Cambridge, Mass., Dec., 1980.